ADVANCED FUNCTIONAL MATERIALS
www.afm-journal.de

VaporLIFT: On-Chip Chemical Synthesis of Glycan Microarrays

*Alexandra Tsouka, Marco Mende, Jasmin Heidepriem, Pietro Dallabernardina, Manuel Garcia Ricardo, Tobias Schmidt, Klaus Bienert, Peter H. Seeberger, and Felix F. Loeffler**

Laser-induced forward transfer (LIFT) of polymers is a versatile printing method for parallel in situ synthesis of peptides on microarrays. Chemical building blocks embedded in a polymer matrix are transferred and coupled in a desired pattern to a surface, generating peptides on microarrays by repetitive in situ solid-phase synthesis steps. To date, the approach is limited to simple, heat induced chemical reactions. The VaporLIFT method, disclosed here, combines LIFT with chemical vapor glycosylation to rapidly generate glycans on microarray surfaces while maintaining inert, low temperature conditions required for glycosylations. Process design and parameter optimization enables the synthesis of a collection of glycans at defined positions on a glass surface. The synthetic structures are detected by mass spectrometry, fluorescently labeled glycan-binding proteins, and covalent staining with fluorescent dyes. VaporLIFT is ideal for parallel screening of other chemical reactions, that require inert and well-defined reaction conditions.

1. Introduction

Oligosaccharides are the most abundant biopolymers on earth, mediating key functions in organisms.[1] Due to their structural complexity and diversity, the understanding of their role in essential life processes is still limited compared to proteins and nucleic acids.[2] The development of microarray technology has enabled parallel mechanistic and functional studies in genomics and proteomics.[2–9] The in situ chemical synthesis of nucleic acids and peptides in the array format has revolutionized microarray production, and is meanwhile fully automated.[10,11] However, these approaches are not compatible with glycan microarray synthesis, due to the complex synthesis conditions for glycosylations, involving low temperatures and harsh chemicals.

Various methods exist for the immobilization of pre-synthesized oligosaccharides on the microarray format.[12] One of the most versatile methods for microarray fabrication is based on the synthesis of amino-linked glycan collections, using automated glycan assembly (AGA),[13,14] followed by covalent attachment of a terminal amine on *N*-hydroxysuccinimide (NHS) functionalized slides.[15] AGA has provided access to several biologically and structurally interesting carbohydrate families of varying lengths, substitution patterns, and complexity.[16–22] Ink-jet printing of the synthetic glycans onto a solid support allows for high-throughput screening of carbohydrate-binding macromolecules, such as proteins, viruses, bacteria, yeast or even mammalian cells.[23–26] Chemical synthesis of glycans via AGA produces one single oligosaccharide at a time, making parallel on-chip synthesis of glycans desirable, analogous to peptides and oligonucleotides.

To date, few methods for on-chip glycan synthesis of microarrays have been reported. Seminal work by Mrksich[27] enabled the manual on-chip chemical synthesis of 24 different disaccharides for subsequent enzymatic modification. On-chip enzymatic synthesis approaches[28,29] include the synthesis of Globo H oligosaccharides.[28] A pH-dependent DNA linker allowed for controlled immobilization, isolation, and purification of the glycan moieties at each step. These proof-of-principle methods, still face on-chip limitations of low throughput, and availability of glycosyl transferases.

The VaporLIFT method for parallel in situ chemical synthesis of glycan microarrays (**Figure 1**) allows the parallel synthesis of different glycans. This method combines the high-throughput capabilities of laser-induced forward transfer (LIFT)[30] with the vapor synthesis method (vaporSPOT) for the parallelization of chemically demanding reactions.[31] LIFT can generate spot patterns containing matrix-embedded chemical building blocks (BBs) on a solid support with high precision, but is limited to

A. Tsouka, M. Mende, J. Heidepriem, P. Dallabernardina, M. Garcia Ricardo, T. Schmidt, K. Bienert, P. H. Seeberger, F. F. Loeffler
Department of Biomolecular Systems
Max Planck Institute of Colloids and Interfaces
Am Muehlenberg 1, 14476 Potsdam, Germany
E-mail: felix.loeffler@mpikg.mpg.de

A. Tsouka, J. Heidepriem, P. H. Seeberger
Institute of Chemistry and Biochemistry
Freie Universität Berlin
Arnimallee 22, 14195 Berlin, Germany

The ORCID identification number(s) for the author(s) of this article can be found under https://doi.org/10.1002/adfm.202310980

DOI: 10.1002/adfm.202310980

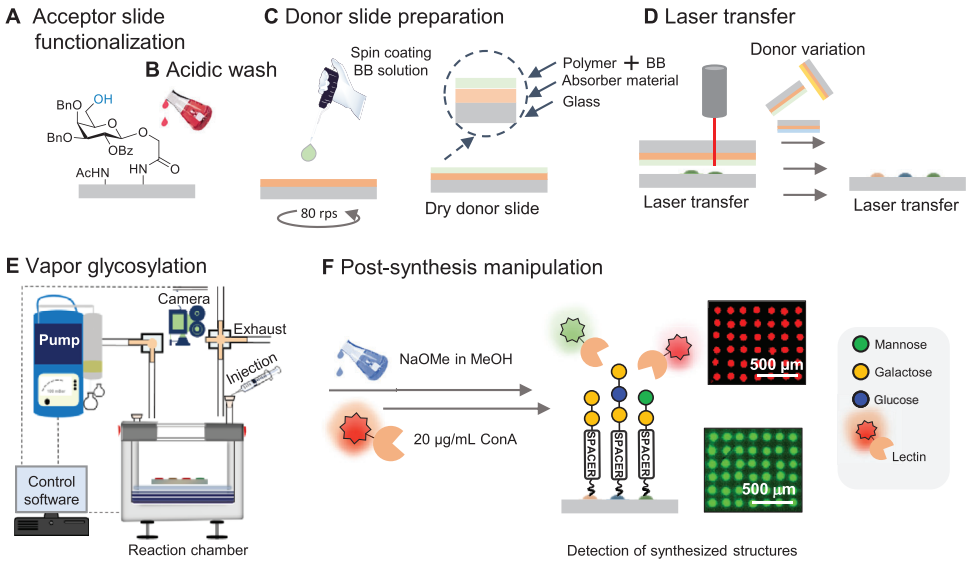

Figure 1. Schematic representation of the VaporLIFT process. A) Functionalization of acceptor glass slide; B) Acidic wash of the functionalized acceptor; C) Preparation of glycosyl donor slides via spin coating. BB: building block. D) Transfer of the glycan BB in polymer matrix by LIFT. E) Computer-controlled vapor glycosylation setup with vacuum pump, cooled reaction chamber, camera, injection and exhaust valve. F) Post-synthesis manipulation; deprotection and validation with fluorescently labeled lectins.

robust reactions such as amide bond formation. In contrast, the vapor synthesis method enables parallelization of temperature and moisture-sensitive chemical glycosylation reactions, but is limited in throughput. Glycosylating agents need to be spotted manually onto individual centimeter-sized membrane pieces. Subsequently, parallel activation and glycosylation of the BBs is achieved by reaction in a dedicated chamber, introducing an activator vapor under controlled conditions.

VaporLIFT allows for the transfer of matrix-embedded glycosylating agents onto a solid support under ambient conditions, since the polymer matrix protects the BB from the environment. The glycosylation is initiated after the exposure of the pattern to the activator vapor under controlled conditions. The main obstacle was the miniaturization of the vapor synthesis approach, enabling glycosylation of the transferred BB patterns on the solid support, while preventing spreading. By thorough process design and parameter optimization, the synthesis of different di- and trisaccharides on a functionalized glass solid support is presented. The synthesized structures are characterized by staining with fluorescently labeled plant lectins, covalent attachment of dyes, and matrix-assisted laser desorption/ionization time-of-flight (MALDI-ToF) mass spectrometry.

2. Results and Discussion

2.1. Design of Solid Support and Building Blocks for VaporLIFT Glycosylation

The VaporLIFT synthesis (Figure 1) begins with the functionalization of a commercially available 3D amino glass slide with the galactopyranoside linker **1** (**Scheme 1**), bearing an Fmoc-protecting group on the C-6 position. Linker **1** was synthesized using commercially available thioglycoside **2**. Glycosylation reaction of thioglycoside **2** with allyl 2-hydroxyacetate,[32] promoted by *N*-iodosuccinimide (NIS) and a catalytic amount of triflic acid (TfOH), afforded derivative **3** in 57% yield. Allyl-deprotection in the presence of tetrakis (triphenyl-phosphine) palladium(0) [$Pd(PPh_3)_4$], afforded the targeted galactosyl linker **1** in 76% yield (Scheme 1A).

A variety of commercially available glass slides were tested regarding their stability under the conditions used in carbohydrate chemistry. Different functionalization approaches of the acceptor glass slide were investigated with and without spacer prior to linker **1** attachment, to find the optimum solid support functionalization for array synthesis and detection (see Section SE, Supporting Information). After thorough investigation and optimization, linker **1** is directly attached on specific amino-functionalized acceptor glass slides (3D amino slides, Polyan GmbH, Germany). Attachment of linker **1** was achieved by forming an amide bond, while the unreacted free amino groups of the solid support were acetylated resulting in the acceptor glass slide **4** (Scheme 1B). After Fmoc cleavage, the free hydroxyl group on the C6-position of the galactopyranoside linker served as nucleophile for the first glycosylation. An acidic wash was required to remove any residual base (Scheme 1B) prior to any subsequent steps. Donor slides were prepared by spin coating the solution of the desired glycan BB together with a polymer matrix (Figure 1C).

Perbenzoylated trichloroacetimidate mannose (Man) building block **6**[33] was selected to develop VaporLIFT, since disaccharide product **7** (Scheme 1C) can be detected via fluorescently labeled lectin Concanavalin A (ConA) following laser transfer, glycosylation, and deprotection of the permanent benzoyl protecting groups. Benzoyl groups were chosen for hydroxyl group protection, as they are more stable than acetate esters during glycosylation reactions. An anomeric trichloroacetimidate leaving group can be obtained in high yield and stereoselectivity, requiring only catalytic amounts of a Lewis acid for activation during glycosylation. The donor slide bearing glycosyl donor **6** was placed on top

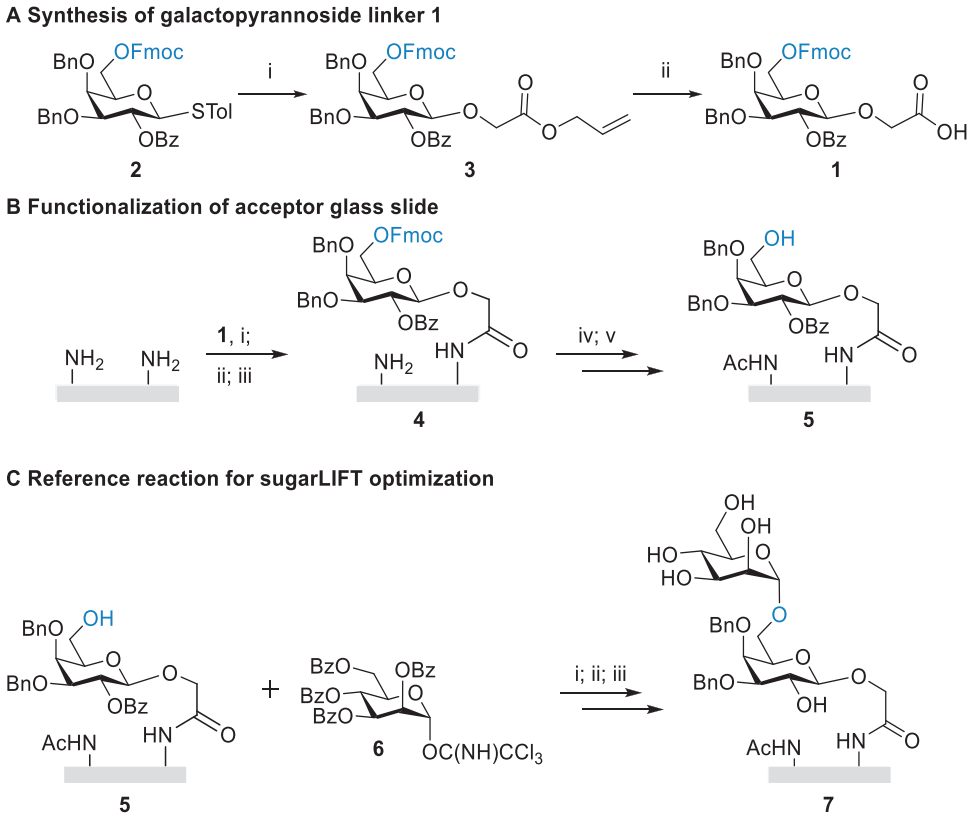

Scheme 1. A) Synthesis of building block 1 for surface functionalization. Reagents and conditions used: i) allyl 2–hydroxyacetate,[32,34] NIS, TfOH, anhydr. dichloromethane (DCM), −20 °C, 1.5 h, 57%; ii) $Pd(PPh_3)_4$, AcOH, THF, rt, overnight, 76%. B) Functionalization of the acceptor glass slide 5. Reagents and conditions used: i) attachment of linker 1, DIC, HOBt, anhydr. DMF, rt, overnight; ii) 10% Ac_2O, 20% DIPEA in DMF (v/v), rt, 30 min (× 2); ii) 10% Ac_2O, 2% MsOH in DCM (v/v), rt, 30 min (× 2); iv) 20% piperidine in DMF(v/v), rt, 20 min; v) acidic wash using 0.5% TMSOTf in DCM (v/v), rt, 1 min. C) Reference reaction for the optimization of the VaporLIFT process. Reagents and conditions used for the synthesis of 7: i) laser transfer of building block 6; ii) glycosylation; iii) deprotection of the ester protecting groups using NaOMe in MeOH.

of the acceptor slide **5** and mounted for a gradient laser transfer inside the laser synthesizer. After vapor glycosylation, each slide was washed, deprotected overnight in a basic solution, and stained with ConA to visualize the product.

2.2. Optimization of VaporLIFT

The robotic LIFT synthesis of peptide microarrays[35] follows the Fmoc-based solid phase peptide synthesis developed by Merrifield,[36] where coupling of the transferred building blocks is achieved by heating to 95 °C for 10 min. After washing, capping, and deprotection, the next building block layer can be coupled. These conditions are incompatible with the chemical synthesis of carbohydrates. Initial vapor glycosylation of the transferred mannose building block **6** failed, when using the previously reported vapor glycosylation setup and conditions.[31] We hypothesized that this failure was a result of the glass vapor glycosylation chamber and the limited cooling capacity of the air-cooled thermoelectric element. The glass wall shields the glass solid support and prevents direct cooling. To overcome this problem, we designed a larger and more powerful reaction chamber (Figure 1C; Section SF, Figures S5 and S6, Supporting Information) to contain a full microscope slide (2.5 × 7.5 cm^2). A 7.5 × 7.5 cm^2 metal cooling plate was implemented for direct thermal contact to a more powerful water-cooled thermoelectric element in a chamber. A window in a heatable lid, preventing undesired condensation, enables observation of the vapor process (Section SF, Videos S1 and S2, Supporting Information). Screening various parameters in numerous model glycosylation reactions in the new setup showed first successful glycosylation results (Figure S4, Supporting Information), but showing large reproducibility issues with strong diffusion, deformation, and spreading of the desired patterns.

Throughout the technical and chemical optimization of the VaporLIFT method, an empirical fluorescence-based approach was implemented. Since the aromatic protecting groups fluoresce, a fluorescence scanner was used to validate the acceptor functionalization as well as the successful laser transfer and pattern stability during and after the VaporLIFT process (see Section SP, Supporting Information).

Many different parameters had to be controlled for the vapor generation, requiring argon bubbling through 1 mL of temperature-controlled activator solution. To simplify vapor generation, prior to the injection of the activator solution, the reaction chamber was evacuated under high vacuum by connecting to the Schlenk line. The activator solution was evaporated and eventually condensed on the solid support, initiating the

glycosylation. Different amounts of activator solution and syringes were tested. Precise injection of 30 µL of activator solution with a Hamilton syringe resulted in improved results, but still showed some pattern deterioration. We found that the vacuum slowly dissipated uncontrollably from the chamber after disconnecting the high vacuum. Delayed injection after evacuation improved the results further, but was difficult to control. For more precise pressure control a vacuum pump was included in the final technical setup (Figure 1E).

For method development, chemical parameters were thoroughly optimized. Initially, different vacuum pressures (50, 100, and 200 mbar, see Section SH, Supporting Information) were evaluated under the same glycosylation conditions. The vacuum was applied to the system, while the reaction chamber was cooled to −5 °C. The glycosyl donor was activated by injecting 30 µL of 20% TMSOTf in DCM, which was maintained at −5 °C for 30 min. After completion, the remaining condensate was removed from the glycosylation chamber under high vacuum and the temperature increased to 30 °C. An inverse correlation of pressure and amount of vapor condensing on the slide was observed with the camera and confirmed by evaluation of the lectin staining result. Under higher vacuum (50 mbar), more vapor condensed on the slide, leading to migration and deterioration of the transferred patterns. Vapor glycosylation under lower vacuum (200 mbar) was unsuccessful, since too little vapor condensed to initiate the glycosylation, while at 100 mbar, the transferred pattern was most consistent. This value was chosen for further optimizations.

Next, three different amounts of activator solution were injected (60, 70, and 100 µL; Section SH, Supporting Information). A 70 µL injection showed optimum stability of the transferred pattern, whereas the other amounts resulted in high background noise or no distinguishable pattern.

As described above, the temperature was maintained at –5 °C for 30 min and afterward, the temperature was rapidly increased to 30 °C. While the starting temperature of −5 °C was already optimal, instead of maintaining the temperature at –5 °C for 30 min, we investigated heating gradients from –5 to 30 °C, directly after injection (1 or 7 °C min^{-1}; Section SH, Supporting Information). The slow temperature gradient resulted in pattern deterioration, while the faster gradient significantly increased the fluorescence signal and pattern stability.

In addition, the concentration of the activator solution was investigated. Glycosyl trichloroacetimidates require only catalytic amounts of activator for activation. Despite the intense fluorescence signal obtained using 20% TMSOTf in DCM (Section SH, Supporting Information), it was necessary to reduce the amount of Lewis acid used to minimize potential side reactions, while ensuring sufficient activation of the glycosylating agent. Five different concentrations of activator (5%, 10%, 15%, and 20%) in DCM were tested. Using 5% TMSOTf in DCM, no successful glycosylation was observed, while 10% and 15% resulted in similar fluorescence intensities upon lectin staining. Thus, 10% was sufficient for activation of the building block.

Different building blocks and polymer concentrations were investigated for cost-effective donor slide preparation. Reducing both, the amount of glycosylating agent and polymer matrix, resulted in only slightly lower fluorescence intensities (Section SH, Supporting Information). To ensure protection of the BB by a sufficiently thick polymer layer from the heat generated during LIFT and environmental moisture, 5 mg of BB **6** were mixed in 25 mg of polymer matrix in 500 µL DCM for one donor slide.

For lectin staining, deprotection of the benzoyl groups with sodium methoxide and potassium carbonate in methanol was investigated. Sodium methoxide was selected, since the low solubility of potassium carbonate in methanol results in scratches on the functionalized glass surface (see Figure S4, Supporting Information). Validation of disaccharide **7** was accomplished after selective staining with fluorescently labeled ConA (red fluorescence channel, excitation 635 nm). The final lectin concentration for staining was reduced to 20 µg mL^{-1}. All further studies were performed under the optimized conditions (**Figure 2**).

2.3. Validation by Mass Spectrometry

Encouraged by the reproducible synthesis and detection of disaccharide **7** patterns via ConA, product validation by mass spectrometry (MS) via two different approaches was explored: glycosylation in solution on the glass solid support (**Scheme 2A**; Sections SJ and SK, Supporting Information) and via laser transfer (Scheme 2B) in our custom-built vapor setup under the optimized conditions. First, a commercial photocleavable linker (see Section SE, Supporting Information) was covalently attached via amide bond to the slide prior to linker **1** and glass slide **8** was subjected for in solution glycosylation under inert conditions in a glass chamber (Figure S8, Supporting Information) using excess mannopyranoside **6**. Detection of disaccharide product **9** was achieved after cleavage under UV-light irradiation (365 nm) and analysis by MALDI-ToF MS. For direct glycosylation without prior attachment of a sugar moiety on the solid support, another photocleavable linker was synthesized,[31] and covalently attached to the amino-functionalized glass slide (Section SE, Supporting Information). Acceptor slide **10** was glycosylated after transfer of glycosylating agent **6** over the entire acceptor slide, followed by vapor glycosylation. The result was validated by in situ MALDI-ToF MS on the glass slide for the detection of monosaccharide **11**. Further characterization of the compounds was not possible due to low yield from the solid support (Section SK, Supporting Information).

2.4. Parallel VaporLIFT Synthesis

To show the versatility of the vapor glycosylation, simultaneous glycosylation reactions of different glycosylating agents on the same solid support were investigated. A collection of BBs was synthesized, either following established protocols (**12, 13, 15–20**)[31,37–39] or prepared from commercially available precursors (**Figure 3A**; Section SD, Supporting Information, for mannopyranoside **14**). Each BB contains permanent protecting groups such as benzyl ethers, benzoyl esters, as well as temporary Fmoc and Lev protecting groups to identify candidates for chain elongation with good glycosylation efficiency.

Ten different donor slides bearing building blocks **6** and **12–20**, were prepared for the parallel synthesis and transferred on substrate **5** in a gradient pattern, varying the lasing power and duration with our automated system.[35] Lasing parameters were in

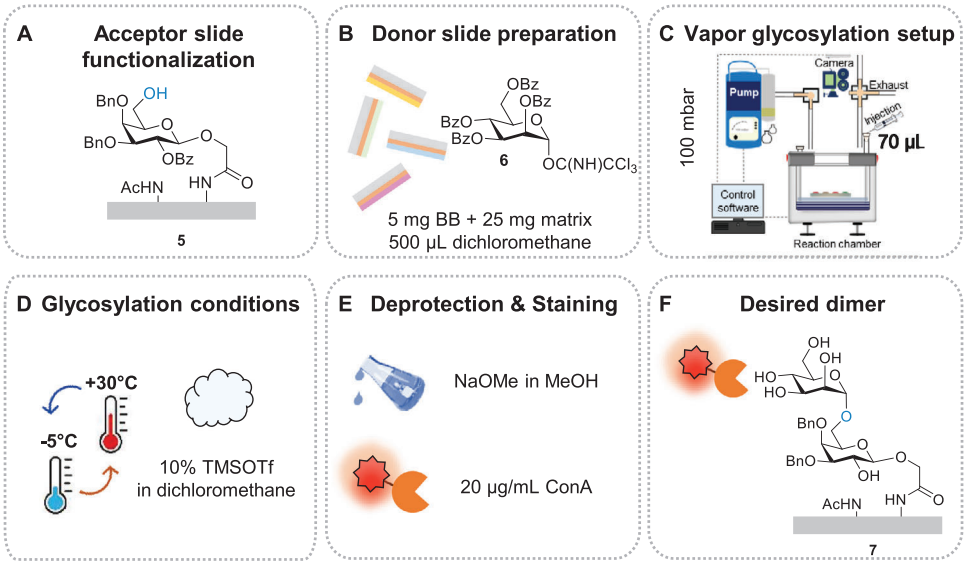

Figure 2. Optimized VaporLIFT parameters. A) The microarray is functionalized with a linker containing a glycosyl acceptor. B) The donor slide is prepared with 5 mg BB in 25 mg polymer. C,D) The pressure in the glycosylation chamber is set to 100 mbar and 70 µL of 10% TMSOTf in DCM is injected, while the heating starts from −5 to 30 °C with a rate of 7 °C min^{-1}. E) Deprotection of the protecting groups is performed in NaOMe in MeOH, and fluorescent-lectin staining with 20 µg mL^{-1} ConA. F) Screening of the formed dimer 7 via fluorescent scan.

the range of 110–190 mW and 21–25 ms per spot, with a spot density of 100 cm^{-2}. Perbenzoylated mannose building block **6** was used as a positive control and building block **13** as a negative control, bearing permanent benzoyl protecting groups on the C-3 and C-4 positions. The ester and carbonyl protecting groups (-Bz, -Fmoc, -Lev) can be readily removed under basic conditions for lectin recognition. A single simultaneous vapor glycosylation on the functionalized glass slide with mannopyranosides **6**, **12–15**, followed by deprotection and ConA staining, showed successful synthesis of disaccharide **7**. Promising candidates were identified for chain elongation, while repetition of the glycosylation process (double coupling) was required for BBs **12** and **15** for successful staining. Glycosyl imidate **14** was identified as a good candidate from the first glycosylation cycle and double glycosylation was not required. However, mannopyranoside **13** unexpectedly gave a positive fluorescence signal, leading to the consideration that the used 10% TMSOTf in DCM solution might be too acidic, potentially leading to acidic cleavage of the benzyl groups (Figure 3B). Despite the successful glycosylation observed for the synthesized mannopyranosides, lectin staining reproducibility issues were encountered with glucopyranosyl imidates **16** and **17**. For these two BBs, single and double glycosylation cycles were implemented. However, after acceptor glass slide **21** was subjected to deprotection, no ConA staining was observed (Figure 3B). Therefore, we followed a covalent validation approach as detailed in the next section. For the terminal galactopyranoside BBs **18–20**, after single glycosylation and Ricinus communis agglutinin–I (RCA–I) staining, galactopyranoside dimer **22** and the trisaccharide **23** were not recognized by the lectin. Repetition of the glycosylation cycle, deprotection and staining of the formed structures with the same lectin showed that all target structures can be successfully recognized by the lectin(s). Future investigations into repetitive glycosylations will have to rule out potential side products and may require further

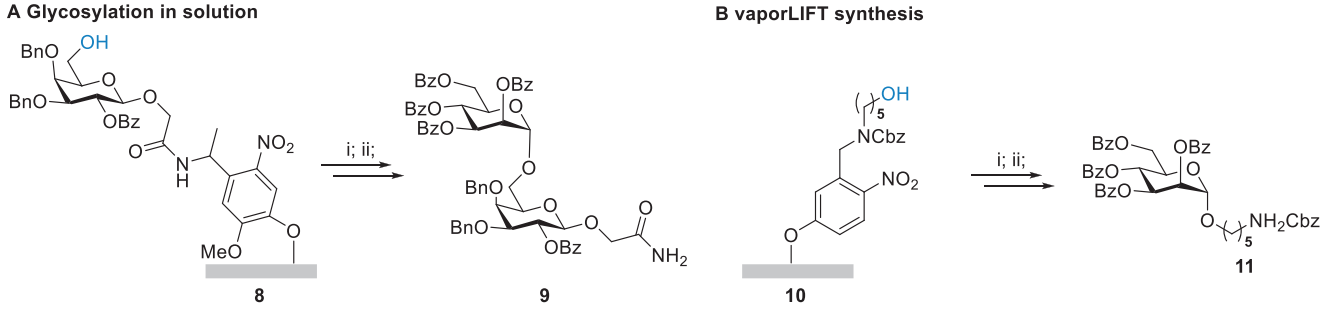

Scheme 2. A) Glycosylation reaction in solution under inert conditions on acceptor glass slide 8, functionalized with a photocleavable linker. Disaccharide 9 was characterized by MALDI. Reagents and conditions: i) Man 6 (30 mg), TMSOTf, DCM, −15 °C to rt, 30 min; ii) cleavage under UV-light irradiation (365 nm), 30 min prior to MALDI detection. B) VaporLIFT synthesis of monosaccharide 11 using the optimized conditions on a functionalized acceptor slide 10. Monosaccharide 11 was detected by in situ MALDI. Reagents and conditions: i) Man 6 transferred via laser transfer on the glass solid support; ii) vapor glycosylation reaction, 10% TMSOTf in DCM, −5 °C to 30 °C, 30 min; iii) direct detection via in situ MALDI.

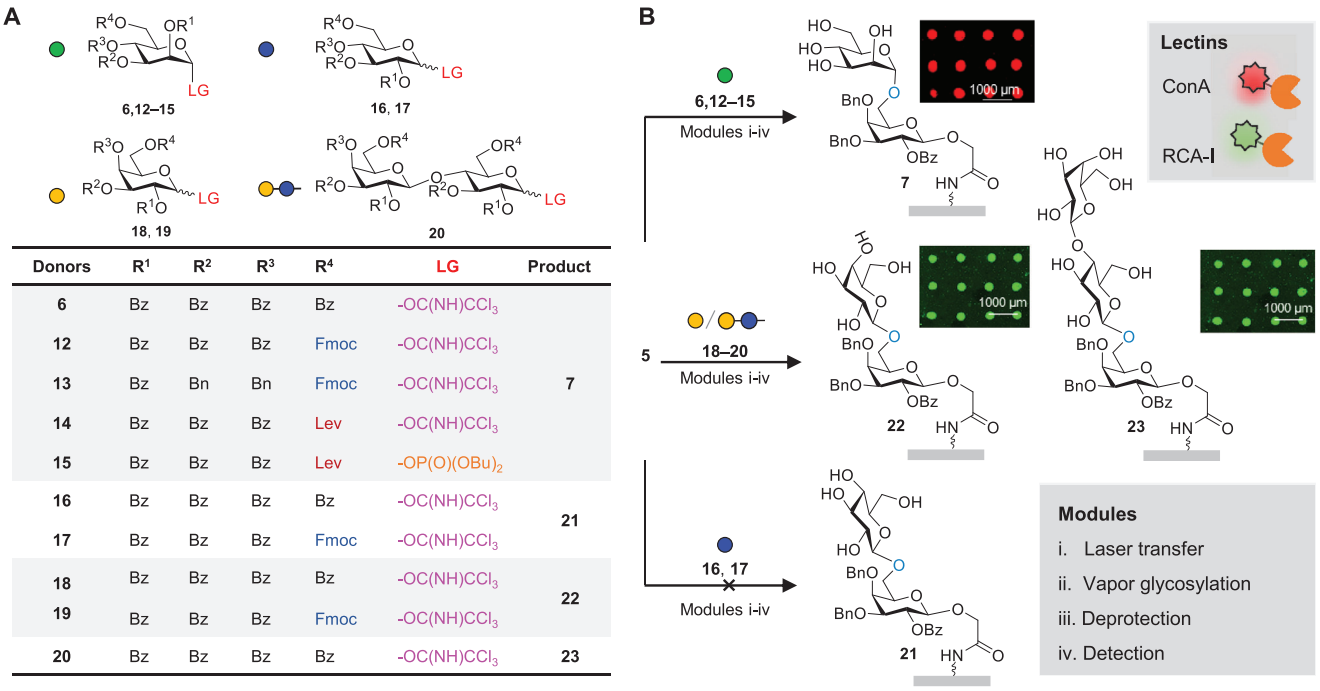

Donors	R^1	R^2	R^3	R^4	LG	Product
6	Bz	Bz	Bz	Bz	$-OC(NH)CCl_3$	
12	Bz	Bz	Bz	Fmoc	$-OC(NH)CCl_3$	
13	Bz	Bn	Bn	Fmoc	$-OC(NH)CCl_3$	7
14	Bz	Bz	Bz	Lev	$-OC(NH)CCl_3$	
15	Bz	Bz	Bz	Lev	$-OP(O)(OBu)_2$	
16	Bz	Bz	Bz	Bz	$-OC(NH)CCl_3$	21
17	Bz	Bz	Bz	Fmoc	$-OC(NH)CCl_3$	
18	Bz	Bz	Bz	Bz	$-OC(NH)CCl_3$	22
19	Bz	Bz	Bz	Fmoc	$-OC(NH)CCl_3$	
20	Bz	Bz	Bz	Bz	$-OC(NH)CCl_3$	23

Figure 3. A) Synthesized building blocks for VaporLIFT synthesis. B) Parallel VaporLIFT synthesis of disaccharides 7, 22 and trisaccharide 23, synthesized from mannosyl 6, 12–15, galactosyl 18–19, and lactosyl donor 20, respectively. Screening of the synthesized structures achieved with their corresponding fluorescently labeled plant lectins (ConA staining represented in red and RCA-I staining in green). Disaccharide 21 was not detected after glycosylation with 16 and 17 and staining with ConA (17 was validated by covalent dye staining). Reagents and conditions: i) laser transfer, laser power 110–190 mW, pulse duration 21–25 ms; ii) vapor glycosylation, 10% TMSOTf in DCM, vacuum 100 mbar, −5 °C to 30 °C, 30 min; iii) NaOMe in MeOH, rt, overnight; iv) ConA (20 µg mL^{-1}) and RCA-I (10 µg mL^{-1}) staining; Scanning parameters: 635 nm excitation, Photomultiplier (PMT) gain 600, pixel size 5 µm for ConA and 532 nm excitation, PMT gain 400, pixel size 5 µm for RCA–I.

optimization of activator concentration. These results demonstrate that the method is compatible with more complex glycosylating agents in the future (Figure 3B).

Finally, to further validate the VaporLIFT glycosylation approach and to overcome reproducibility issues in lectin staining, glycosyl imidates **12**, **17**, and **19**, bearing the same leaving groups and temporary Fmoc-protecting group, were glycosylated in parallel on-chip using the already optimized conditions. Fmoc-deprotection was followed by Steglich esterification between the free hydroxy group of the C-6 position and a Fmoc-propargylglycine. The successful glycosylation and esterification reaction of all used building blocks was detected via covalent bond formation between the synthesized structures and a fluorescent dye using copper-catalyzed azide-alkyne cycloaddition (CuAAC) as reported in the literature[41,42] (see Section SM, Supporting Information). In addition, to verify the versatility of our vaporLIFT method, two additional glycosyl phosphate building blocks were synthesized for direct labeling via CuAAC and amide bond formation[35] respectively. Staining with the corresponding fluorescent dyes (TAMRA-azide and DyLight 633-B2 NHS ester) revealed a successful glycosylation of both building blocks on chip (see Sections SN and SO, Supporting Information).

3. Conclusion

The VaporLIFT method was developed for on-chip parallel chemical synthesis of glycans under inert and temperature-controlled conditions. A custom-built vapor glycosylation setup was designed and process parameters were optimized. We investigated the laser transfer parameters, the required vapor glycosylation conditions, and developed an efficient deprotection protocol, to ensure successful glycosylation and detection, while maintaining the desired pattern. The VaporLIFT method is the first parallel on-chip chemical synthesis of oligosaccharides automatically maintaining low temperature for stereochemical control in an inert environment. Detection and validation of the glycan products was performed by mass spectrometry, non-covalent lectin staining, and covalent staining via fluorescent dyes.

Further optimization of this method, including other BBs and leaving groups, will lead to more complex and branched structures, with different protecting groups, opening a path to high-throughput synthesis of *O*- and *N*-glycans or glycopeptides on-chip.

The use of an automated laser-based synthesizer[35] and the newly developed hematite absorber for donor generation[40] can further increase parallelization, accelerating the screening of multiple biomolecular interactions.

4. Experimental Section

Preparation of Donor and Acceptor Slides: *Donor Slide*: Microscope glass slides (Marienfeld Superio, Germany; size 76 × 26 × 1 mm, ground edges, pure white glass) were covered on one side with self-adhesive polyimide foil (Kapton, DuPont, USA, CMC Klebetechnik GmbH, Germany;

thickness of polyimide layer approximately 25 µm, thickness of glue layer approximately 45 µm). A thin layer of the transfer material was placed on top of the polyimide foil by spin coating (80 rps, Schaefer Technologie GmbH, Germany; KLM Spin Coater SCC-200). All spin coating solutions were prepared in the same way. Glycosyl donors (5.00 mg), and inert polymer matrix (25 mg) (SLEC PLT 7552, Sekisui Chemical GmbH, Germany) were dissolved in dichloromethane (DCM) (500 µL), resulting the spin coating solution.

Acceptor Slide: The 3D-Amino glass slides (according to vendor 1–5 nmol cm^{-1}) were obtained from PolyAn GmbH, Berlin, Germany. For in situ chemical synthesis slides were functionalized for lectin screening with one galactopyranoside BB while for MALDI-ToF two different functionalizations were acquired a) with a commercially available photocleavable linker and the galactopyranoside BB and b) with a photocleavable linker for direct glycosylation. For further information, please see Supporting Information.

Laser Transfer Parameters: *For Process Optimization*: A laser scanning system with 488 nm wave-length and 120 mW maximum output power was used,[41,42] with a laser focus diameter of ≈20 µm. A laser power of 80 mW with a pulse duration range of 20–27.5 ms was applied for the optimization experiments.

For VaporLIFT Glycosylation: A laser scanning system with 488 nm wavelength and 120 mW maximum output power was used,[41,42] with a laser focus diameter of ≈20 µm. A laser power of 80 mW with a pulse duration range of 20 ms was applied.

For Parallel Synthesis: For the array synthesis, a spot pitch of 1 mm was used. A laser scanning system with 405 nm wavelength and 210 mW maximum output power with a laser focus diameter of 50 µm was used.[35] The automated transfer of the donor slides to the acceptors, placed in the slide holder with a robot with 20 µm precision. A laser gradient from 110 to 190 mW was applied with a pulse duration range of 20–25 ms.

Laser Transfer System for Method Optimization: The laser system consists of a 200 mW TOPTICA iBeam smart 488-S laser with a wavelength of 488 nm (TOPTICA Photonics, AG, Gräfelfing/Bayern, Germany), which is passed through a 1:10 beam expander and a Racoon 11 laser scanning system (ARGES GmbH, Wackersdorf/Bayern, Germany), equipped with an f-Theta lens (S4LFT5110/322, Sill Optics GmbH, Wendelstein/Bayern, Germany). High quality laser transfer with reproducible 60 results at various positions is achieved with scanning the laser beam in a 66 mm × 66 mm plane. The acceptor slide in the lasing areas was aligned with three mechanical springs and a vacuum mechanism.[41]

Laser Transfer System for Parallel Synthesis: The lasing system consists of a 405 nm wavelength diode laser with a Gaussian beam profile and a maximum of 300 mW power (iBeam smart 405-S, TOPTICA Photonics AG), lead through a laser scanning system (intelliSCAN III 10, SCANLAB), linked to an f-theta- lens (JENar 170-355-140, JENOPTIK Optical Systems GmbH). The measured maximum power in the lasing area is 210 mW. Transport of donor slides between the slide holder and the lasing area is achieved with a KUKA AGILUS six KR 3 R540 robot (KUKA AG), with 20 µm precision. A robot tool, a gripper (with four 2 mm diameter rubber suction cups) is incorporated connected to a pneumatics system that initiates and releases vacuum for transportation. Within the lasing area, simple pressure is produced to ensure mechanical alignment, controlled by the pneumatics system. A strong vacuum (−80 kPa) suction is applied to keep the acceptor slide in place during the process.[35]

Vapor Glycosylation Setup: The optimized vapor glycosylation setup (Figure 1C) consisted of six components: a reaction chamber; a Hamilton syringe; a vacuum pump (PC 3001, VARIO, Vacuubrand GmbH & Co KG, Wertheim, Germany); two valves; a camera to visualize the deposition of the activator solution, and a computer system for temperature regulation of the glycosylation chamber. The temperature is ensured inside and on top (lid) of the chamber by a software installed on a computer. The two valves provide control over the atmosphere inside the setup. The left one is responsible for the applied vacuum from the vacuum pump and the right one for the atmosphere inside the setup after the completion of the glycosylation reaction (air, high vacuum and argon from the Schlenk line). The vapor of the activator solution is formed after injection of the desired amount via a Hamilton syringe. The progress of the entire process is visualized through a window in the lid by a camera placed on top of the reaction chamber, which is connected with the control software. Further details about the technical characteristics of our custom-built setup, the temperature profile and the regulation system can be found in Supporting Information.

General VaporLIFT Process: The laser transfer and the oligosaccharide synthesis was conducted as previously reported in the literature for peptides.[30,35,41,42] The process begins with the preparation of different glycosyl donor slides that are readily prepared by spin coating a solution of polymer matrix and glycosyl donor BB onto the polyimide absorbing foil (Kapton) on microscope glass slides. For the patterning process, a donor slide bearing the desired glycosyl donor is placed on top of a functionalized acceptor slide and a focused laser transfers the desired number of spots (every spot consists of glycosyl donor-solid polymer matrix) from the donor to the acceptor. The polyimide foil absorbs the laser energy and it heats up leading to each expansion. Eventually, the expanding polyimide, touched the surface of the acceptor slide, transferring of nanometer thin spots. The transfer is repeated with different donor slide in different defined positions. Afterward, the acceptor slide is placed into our vapor glycosylation setup (see respective section) and cooled to −5 °C while evacuated to 100 mbar (≈30 min). To initiate the vapor glycosylation, 70 µL of 10% TMSOTf-DCM solution were injected, and the temperature was increased from –5 to 30 °C (7 °C min^{-1} temperature ramp rate). Upon completion, the acceptor slide is washed, removing unreacted glycosyl donor-residual polymer, and hydrolyzed glycosyl donor. The glycosylation reaction can be repeated for increased coupling yield and to minimize deletion sequences. Then, deprotection of the permanent benzoyl ester groups is achieved with NaOMe and the result can be screened via fluorescent labeled lectins.

Synthesis of Glycosyl Donor BBs: Glycosyl donor **14** was prepared from a commercially available precursors as reported in Supporting Information, while all remaining glycosyl donors (**6**, **12, 13, 15–20**) where synthesized following already established protocols.[31,33,37–39]

Plant Lectin Assay: Before lectin staining, acceptor slides were incubated with a blocking buffer for 30 min (Rockland, USA; blocking buffer for fluorescent western blotting MB-070). Fluorescently labeled plant lectins, Concanavalin A (ConA; CF633 ConA, Biotium, Inc., USA) was diluted to 20 µg mL^{-1} in lectin buffer (50 mM HEPES, 100 mM NaCl, 1 mM $CaCl_2$, 1 mM $MnCl_2$, 10% blocking buffer, 0.05% Tween 20, pH 7.5), and Ricinus communis agglutinin I, (RCA-I, Rhodamine labeled, Lectin kit 1, Vector laboratories, USA) was diluted to 10 µg mL^{-1} in lectin buffer and incubated for 1 h at rt. Subsequently, each stained well was washed with PBS-T buffer (3 × 3 min). Then, the acceptor slide was rinsed with Tris buffer (1 mM Tris-HCl buffer, pH 7.4) to remove all the remaining salt residues, and dried by a jet of air. Fluorescence scanning was used to detect the lectin binding on the corresponding sugar moieties.

Fluorescence Scan: Molecular Devices microarray scanner, GenePix 4000B, San Jose, USA, was used for the screening of the obtained oligosaccharides. The detection wavelength was $\lambda = 523$ nm (for Rhodamine RCA-I, TAMRA-azide), with photomultiplier (PMT) gain of 500, and $\lambda = 635$ nm (for CF633 ConA, DyLight 633-B2 NHS ester), with PMT gain 600. The laser power was 33% for every measurement and the pixel size was 5 µm for high-resolution scans.

MALDI-ToF Mass Spectrometry: Mass spectra were obtained from a MALDI-ToF autoflexTM (Bruker) instrument. For in-situ/direct MALDI, the slide was placed on a MTP-TLC adapter obtained from Bruker. On the edges between the slide and the adapter small pieces of (≈1 cm^2) of aluminum (3M, aluminum foil tape 425, silver, 75 mm × 55 m, 0.12 mm) and copper foil tape (True Components, 20 m × 50 mm) were placed to increase the conductivity.

Supporting Information

Supporting Information is available from the Wiley Online Library or from the author.

Acknowledgements

The authors thank the Biomolecular Systems Department for technical support, as well as the electronics workshop of the Max Planck Institute of Colloids and Interfaces. In addition, the authors thank Dr. Grigori Paris for his valuable physics, engineering, and data analysis input throughout this work, as well as Eva Settels and Olaf Niemeyer for their help with the analytical methods. Moreover, the authors thank Dr. José Angél Danglad-Flores, Dr. Eric Sletten, and Owen Tuck for their critical input regarding automation and the temperature effect on glycosylation reactions. This research was supported by the German Federal Ministry of Education and Research (BMBF, grant number 13XP5050A) the MPG-FhG cooperation (Glyco3Display), and the Max Planck Society.

Open access funding enabled and organized by Projekt DEAL.

Conflict of Interest

P.H. Seeberger declares a significant financial interest in GlycoUniverse GmbH & Co. KGaA, the company that commercialized AGA synthesis instruments, BBs, and other reagents. F.F.L. is named on a patent related to laser-based microarray synthesis. F.F.L, A.T., M.M., J.H., and P.H.S. are named on a patent related to the presented technology for glycan synthesis. M.G.R., T.S., K.B., and P.D. declare no conflict of interest.

Data Availability Statement

The data that support the findings of this study are available in the supplementary material of this article.

Keywords

glycosylation, high-throughput screening, laser-induced forward transfer, oligosaccharides, parallel

Received: September 12, 2023
Revised: November 28, 2023
Published online: March 1, 2024

[1] A. Varki, R. D. Cummings, J. D. Esko, P. Stanley, G. W. Hart, M. Aebi, D. Mohnen, T. Kinoshita, N. H. Packer, J. H. Prestegard, R. L. Schnaar, P. H. Seeberger, in *Essentials of Glycobiology*, 4th ed., Cold Spring Harbor Laboratory Press, New York, NY, USA, **2022**.
[2] S. Fodor, J. Read, M. Pirrung, L. Stryer, A. Lu, D. Solas, *Science* **1991**, *251*, 767.
[3] J. P. Pellois, X. Zhou, O. Srivannavit, T. Zhou, E. Gulari, X. Gao, *Nat. Biotechnol.* **2002**, *20*, 922.
[4] V. Stadler, T. Felgenhauer, M. Beyer, S. Fernandez, K. Leibe, S. Güttler, M. Gröning, K. König, G. Torralba, M. Hausmann, V. Lindenstruth, A. Nesterov, I. Block, R. Pipkorn, A. Poustka, F. R. Bischoff, F. Breitling, *Angew. Chem. Int. Ed.* **2008**, *47*, 7132.
[5] J. V. Price, S. Tangsombatvisit, G. Xu, J. Yu, D. Levy, E. C. Baechler, O. Gozani, M. Varma, P. J. Utz, C. L. Liu, *Nat. Med.* **2012**, *18*, 1434.
[6] S. Buus, J. Rockberg, B. Forsström, P. Nilsson, M. Uhlen, C. Schafer-Nielsen, *Mol. Cell. Proteomics* **2012**, *11*, 1790.
[7] J. B. Legutki, Z.-G. Zhao, M. Greving, N. Woodbury, S. A. Johnston, P. Stafford, *Nat. Commun.* **2014**, *5*, 4785.
[8] C. Moreno-Yruela, M. Bæk, A.-E. Vrsanova, C. Schulte, H. M. Maric, C. A. Olsen, *Nat. Commun.* **2021**, *12*, 62.
[9] W. Lin, S. Gandhi, A. R. Oviedo Lara, A. K. Thomas, R. Helbig, Y. Zhang, *Adv. Mater.* **2021**, *33*, 2102349.
[10] L. C. Szymczak, H. Y. Kuo, M. Mrksich, *Anal. Chem.* **2018**, *90*, 266.
[11] D. S. Mattes, N. Jung, L. K. Weber, S. Bräse, F. Breitling, *Adv. Mater.* **2019**, *31*, 1806656.
[12] M. Mende, V. Bordoni, A. Tsouka, F. F. Loeffler, M. Delbianco, P. H. Seeberger, *Faraday Discuss.* **2019**, *219*, 9.
[13] O. J. Plante, E. R. Palmacci, P. H. Seeberger, *Science* **2001**, *291*, 1523.
[14] J. Danglad-Flores, S. Leichnitz, E. T. Sletten, A. Abragam Joseph, K. Bienert, K. Le Mai Hoang, P. H. Seeberger, *J. Am. Chem. Soc.* **2021**, *143*, 8893.
[15] A. Geissner, A. Reinhardt, C. Rademacher, T. Johannssen, J. Monteiro, B. Lepenies, M. Thépaut, F. Fieschi, J. Mrázková, M. Wimmerova, F. Schuhmacher, S. Götze, D. Grünstein, X. Guo, H. S. Hahm, J. Kandasamy, D. Leonori, C. E. Martin, S. G. Parameswarappa, S. Pasari, M. K. Schlegel, H. Tanaka, G. Xiao, Y. Yang, C. L. Pereira, C. Anish, P. H. Seeberger, *Proc. Natl. Acad. Sci.* **2019**, *116*, 1958.
[16] A. A. Joseph, A. Pardo-Vargas, P. H. Seeberger, *J. Am. Chem. Soc.* **2020**, *142*, 8561.
[17] Y. Zhu, M. Delbianco, P. H. Seeberger, *J. Am. Chem. Soc.* **2021**, *143*, 9758.
[18] M. G. Ricardo, E. E. Reuber, L. Yao, J. Danglad-Flores, M. Delbianco, P. H. Seeberger, *J. Am. Chem. Soc.* **2022**, *144*, 18429.
[19] T. Tyrikos-Ergas, E. T. Sletten, J.-Y. Huang, P. H. Seeberger, M. Delbianco, *Chem. Sci.* **2022**, *13*, 2115.
[20] G. Fittolani, T. Tyrikos-Ergas, A. Poveda, Y. Yu, N. Yadav, P. H. Seeberger, J. Jiménez-Barbero, M. Delbianco, *Nat. Chem.* **2023**, *15*, 1461.
[21] T. Tyrikos-Ergas, S. Gim, J.-Y. Huang, S. Pinzón Martín, D. Varón Silva, P. H. Seeberger, M. Delbianco, *Nat. Commun.* **2022**, *13*, 3954.
[22] E. T. Sletten, J. Danglad-Flores, S. Leichnitz, A. Abragam Joseph, P. H. Seeberger, *Carbohydr. Res.* **2022**, *511*, 108489.
[23] M. Guberman, M. Bräutigam, P. H. Seeberger, *Chem. Sci.* **2019**, *10*, 5634.
[24] N. Murthy Sabbavarapu, P. H. Seeberger, *J. Org. Chem.* **2021**, *86*, 7280.
[25] P. Dallabernardina, V. Benazzi, J. D. Laman, P. H. Seeberger, F. F. Loeffler, *Org. Biomol. Chem.* **2021**, *19*, 9829.
[26] C. Ghosh, P. Priegue, H. Leelayuwapan, F. F. Fuchsberger, C. Rademacher, P. H. Seeberger, *ACS Appl. Bio Mater.* **2022**, *5*, 2185.
[27] L. Ban, M. Mrksich, *Angew. Chem. Int. Ed.* **2008**, *47*, 3396.
[28] H. R. Heo, K. Il Joo, J. H. Seo, C. S. Kim, H. J. Cha, *Nat. Commun.* **2021**, *12*, 1395.
[29] S. Serna, J. Etxebarria, N. Ruiz, M. Martin-Lomas, N.-C. Reichardt, *Chem. – A. Eur. J.* **2010**, *16*, 13163.
[30] F. F. Loeffler, T. C. Foertsch, R. Popov, D. S. Mattes, M. Schlageter, M. Sedlmayr, B. Ridder, F. X. Dang, C. Von Bojničić-Kninski, L. K. Weber, A. Fischer, J. Greifenstein, V. Bykovskaya, I. Buliev, F. R. Bischoff, L. Hahn, M. A. R. Meier, S. Bräse, A. K. Powell, T. S. Balaban, F. Breitling, A. Nesterov-Mueller, *Nat. Commun.* **2016**, *7*, 11844.
[31] A. Tsouka, P. Dallabernardina, M. Mende, E. T. Sletten, S. Leichnitz, K. Bienert, K. Le Mai Hoang, P. H. Seeberger, F. F. Loeffler, *J. Am. Chem. Soc.* **2022**, *144*, 19832.
[32] A. Wissner, C. V. Grudzinskas, *J. Org. Chem.* **1978**, *43*, 3972.
[33] F. Bien, T. Ziegler, *Tetrahedron: Asymmetry* **1998**, *9*, 781.
[34] C. D. Spicer, M. Pujari-Palmer, H. Autefage, G. Insley, P. Procter, H. Engqvist, M. M. Stevens, *ACS Cent. Sci.* **2020**, *6*, 226.
[35] G. Paris, J. Heidepriem, A. Tsouka, Y. Liu, D. S. Mattes, S. Pinzón Martín, P. Dallabernardina, M. Mende, C. Lindner, R. Wawrzinek, C. Rademacher, P. H. Seeberger, F. Breitling, F. R. Bischoff, T. Wolf, F. F. Loeffler, *Adv. Mater.* **2022**, *34*, 2200359.
[36] R. B. Merrifield, *J. Am. Chem. Soc.* **1963**, *85*, 2149.
[37] M. S. Sandbhor, N. Soya, A. Albohy, R. B. Zheng, J. Cartmell, D. R. Bundle, J. S. Klassen, C. W. Cairo, *Biochemistry* **2011**, *50*, 6753.
[38] S. Rio, J.-M. Beau, J.-C. Jacquinet, *Carbohydr. Res.* **1991**, *219*, 71.

[39] T. Zhang, X. Li, H. Song, S. Yao, *New J. Chem.* **2019**, *43*, 16881.
[40] J. Zhang, Y. Liu, S. Ronneberger, N. V. Tarakina, N. Merbouh, F. F. Loeffler, *Adv. Mater.* **2022**, *34*, 2108493.
[41] M. Mende, A. Tsouka, J. Heidepriem, G. Paris, D. S. Mattes, S. Eickelmann, V. Bordoni, R. Wawrzinek, F. F. Fuchsberger, P. H. Seeberger, C. Rademacher, M. Delbianco, A. Mallagaray, F. F. Loeffler, *Chem. – A. Eur. J.* **2020**, *26*, 9954.
[42] A. Tsouka, K. Hoetzel, M. Mende, J. Heidepriem, G. Paris, S. Eickelmann, P. H. Seeberger, B. Lepenies, F. F. Loeffler, *Front. Chem.* **2021**, *9*, 931.

